

Effect of higher borides and inhomogeneity of oxygen distribution on critical current density of undoped and doped magnesium diboride

This article has been downloaded from IOPscience. Please scroll down to see the full text article.

2010 J. Phys.: Conf. Ser. 234 012031

(<http://iopscience.iop.org/1742-6596/234/1/012031>)

View [the table of contents for this issue](#), or go to the [journal homepage](#) for more

Download details:

IP Address: 128.131.38.71

The article was downloaded on 10/08/2010 at 10:25

Please note that [terms and conditions apply](#).

Effect of higher borides and inhomogeneity of oxygen distribution on critical current density of undoped and doped magnesium diboride

T A Prikhna¹, W Gawalek², V M Tkach¹, N I Danilenko³, Ya M Savchuk¹,
S N Dub¹, V E Moshchil¹, A V Kozyrev¹, N V Sergienko¹, M Wendt²,
V S Melnikov¹, J Dellith², H Weber⁴, M Eisterer⁴, Ch Schmidt²,
T Habisreuther², D Litzkendorf², J Vajda⁵, A P Shapovalov¹, V Sokolovsky⁶,
P A Nagorny¹, V B Sverdun¹, J Kosa⁵, F Karau⁷, A V Starostina¹

¹ Institute for Superhard Materials of the National Academy of Sciences of Ukraine, 2, Avtozavodskaya Str., Kiev 04074, Ukraine

² Institut für Photonische Technologien, Albert-Einstein-Strasse 9, Jena, D-07745, Germany

³ Institute for Problems of Materials Science of the National Academy of Sciences of Ukraine, 3, Krzhyzhanivsky Str., Kiev 03142, Ukraine

⁴ Atomic Institute of the Austrian Universities, 1020 Vienna, Austria

⁵ Budapest University of Technology and Economics, Budapest, Hungary 1111 Budapest, Egrý József u. 18. Hungary

⁶ Ben-Gurion University of the Negev, P.O.B. 653, Beer-Sheva 84105 Israel

⁷ H.C. Starck GmbH, Goslar 38642, Germany

E-mail: prikhna@iptelecom.net.ua, prikhna@mail.ru

Abstract. The effect of doping with Ti, Ta, SiC in complex with synthesis temperature on the amount and distribution of structural inhomogeneities in MgB₂ matrix of high-pressure-synthesized-materials (2 GPa) which can influence pinning: higher borides (MgB₁₂) and oxygen-enriched Mg-B-O inclusions, was established and a mechanism of doping effect on j_c increase different from the generally accepted was proposed. Near theoretically dense SiC-doped material exhibited $j_c = 10^6$ A/cm² in 1T field and $H_{irr} = 8.5$ T at 20 K. The highest j_c in fields above 9, 6, and 4 T at 10, 20, and 25 K, respectively, was demonstrated by materials synthesized at 2 GPa, 600 °C from Mg and B without additions (at 20 K $j_c = 10^2$ A/cm² in 10 T field). Materials synthesized from Mg and B taken up to 1:20 ratio were superconductive. The highest j_c (6×10^4 A/cm² at 20 K in zero field, $H_{irr} = 5$ T) and the amount of SC phase (95.3% of shielding fraction), T_c being 37 K were demonstrated by materials having near MgB₁₂ composition of the matrix. The materials with MgB₁₂ matrix had a doubled microhardness of that with MgB₂ matrix (25 ± 1.1 GPa and 13.08 ± 1.07 GPa, at a load of 4.9 N, respectively).

1. Introduction

Synthesis and sintering of MgB₂ under high pressure conditions allow one to produce near theoretically dense nanostructural material with a good connectivity between grains and a high critical

¹ Institute for Superhard Materials of the NASU, 2, Avtozavodskaya Str., Kiev 04074, Ukraine.

current density, j_c , for a short time. High pressure (1-2 GPa) suppresses the magnesium from being evaporated and prevents grain growth (the average sizes of crystallites estimated by X-ray did not surpass 15-37 nm) [1]. The progress in engineering of high-pressure apparatuses made it possible to synthesize large blocks (in our case above 60 mm in diameter), which makes this method interesting not only from the theoretical point of view.

In 2005 the first SC motor of zebra-type rotor was constructed using high pressure-synthesized (HPS) MgB_2 . The tests showed its competitiveness at liquid hydrogen temperatures (15-20 K) with motor based on MT-YBCO, besides the high pressure-synthesized MgB_2 is two-three times lower in cost and easier in production than MT-YBCO [2]. The first investigations of high pressure-synthesized MgB_2 rings for inductive fault-current limiters in the Ben-Gurion University of the Negev (by V. Meerovich and V. Sokolovsky) showed encouraging results: the transition is very fast, cylinders can provide higher impedance change at the transition from nominal to limiting regime.

Due to the comparatively large coherent length (1.6-12 nm) pinning centres in MgB_2 can be grain boundaries and nanosized inclusions. Because of this, high j_c can be attained in nanocrystalline material and superconducting (SC) properties can be improved by alloying with nanosized properly distributed grains of additives. The atomic resolution study of oxygen incorporation into the bulk MgB_2 [3] shows that 20-100 nm sized precipitates of $\text{Mg}(\text{B},\text{O})$ are formed by ordered substitution of oxygen atoms to boron lattice sites, while the basic bulk MgB_2 crystal structure and orientation are preserved. The periodicity of the oxygen ordering is dictated by the oxygen concentration in the precipitates and primarily occurs in the (010) plane [3]. The presence of these precipitates correlates well with an improved critical current density and superconducting transition behavior, implying that they act as pinning centres [3].

Our previous study has established that superconductive properties of high pressure manufactured MgB_2 depend on the amount, size and distribution of higher borides inclusions with near MgB_{12} stoichiometry (the finer the MgB_{12} grains and the larger amount of them, the higher j_c) [4]. Besides, it has been shown that additions of Ti, Ta, and Zr can improve critical current density j_c , (Fig.1) upper critical field, B_{c2} , and irreversibility line, IL, of high-pressure high-temperature synthesized MgB_2 [5], but we did not observe the same mechanism as it was described for magnesium diboride obtained under normal pressure conditions [6]. In case of adding Ti or Zr the improvement in critical current density in materials synthesized at ambient pressure was usually explained by the formation of TiB_2 or ZrB_2 thin layers or inclusions at grain boundaries of MgB_2 that increase the number of pinning centres, which is ascribed to a j_c improvement caused by doping with these elements [6]. In high-pressure synthesized MgB_2 , the Ti-, Zr- or Ta-containing inclusions are rather coarse (Fig. 2) and randomly distributed in the matrix material to be pinning centres by themselves or to refine the MgB_2 structure. Under high pressure Zr, Ti or Ta absorb impurity hydrogen (the source of which can be materials of high-pressure cell surrounded the sample during synthesis) to form $\text{TiH}_{1.94}$, ZrH_2 , or Ta_2H (Fig. 3a, b, c), thus preventing the harmful (for j_c) MgH_2 (Fig. 3d) impurity phase from appearing and hydrogen from being introduced into the material structure. Besides, it has been observed that the presence, for example, of Ti or Ta promotes the formation of MgB_{12} inclusions, which positively affect pinning in MgB_2 -based materials (Table. 1), while the appearance of ZrB_2 in the structure does not affect the j_c of HPS MgB_2 -based ceramics (Fig. 4). Ti- and Zr-doped HPS-synthesized materials demonstrated extremely high upper critical fields and (at 20 K $B_{c2} = 12.5$ T and 11 T and $H_{irr} = 9$ T and 8 T for the cases of Ti and Zr additions, respectively) and rather high j_c , which practically were not increased by irradiation [5]. The study of high pressure-synthesized material from Mg and B with 10% of Ti addition (the j_c dependences, structure and X-ray pattern of which shown in Figs. 1, 2, 3b) by SIMS chemical analysis using a Cameca NanoSIMS 50 with a Cs^+ primary ion beam (with possibility to map the hydrogen distribution in the specimens) and by Electron Microprobe analysis (EPMA) using a JEOL JXA 8800 Superprobe as well as by transmission electron microscopy on powdered samples dispersed on a lacy carbon film using a JEOL 3000F HR-TEM fitted with an energy dispersive X-ray (EDX) detector has shown that the only Ti-containing phase in the material was $\text{TiH}_{1.924}$ [7] despite the fact that the enthalpy of titanium oxides formation is lower than that of TiH_2 .

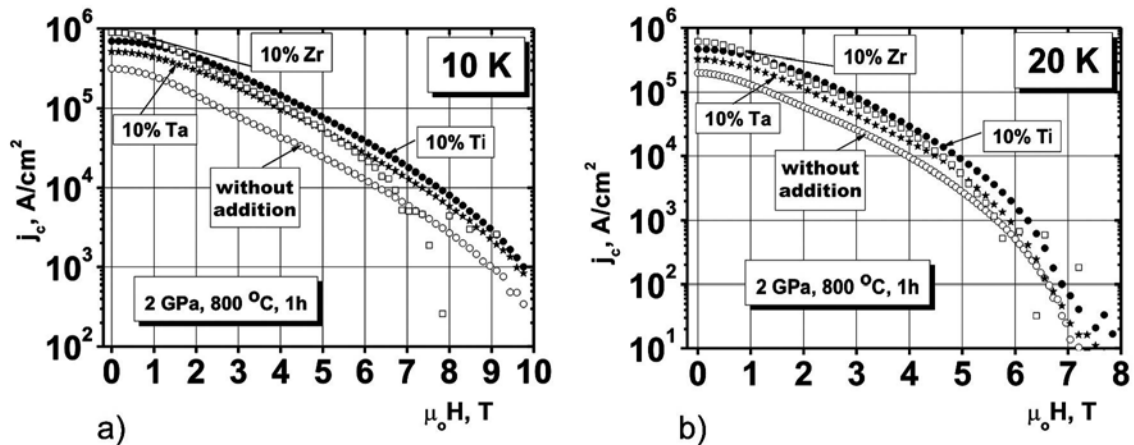


Figure 1. (a, b) Dependences of critical current density, j_c , on magnetic fields, $\mu_0 H$ for HPS-materials at 2 GPa, 800 °C for 1 h prepared from Mg:B(IV)=1:2 without additions and with additions of 10 wt% of Ti, Ta and Zr at 10 K (a) and 20 K (b).

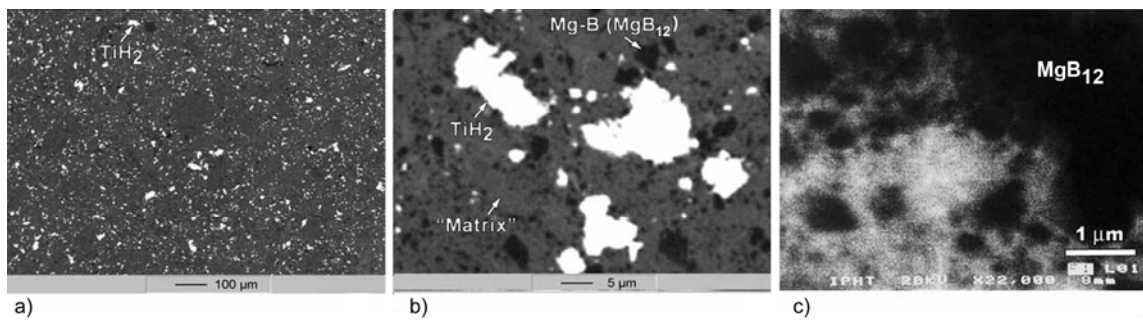


Figure 2. Structures (a, b, c) of high-pressure synthesized material from Mg:B(IV)=1:2 with 10 wt% of Ti at 2 GPa, 800 °C for 1 h at different magnifications (obtained using SEM, “composition” or backscattering electron images, in which the heavier element, the brighter it looks).

Table 1. Critical current density, j_c , vs. relative amount, N , of “black inclusions” with near MgB₁₂ stoichiometry in high-pressure synthesized samples from Mg and B(IV) taken in MgB₂ stoichiometry (or in 1:2 ratio).

Manufacturing parameters: pressure, P , temperature, T , holding time, τ ,	Name of addition, and its amount, wt%	j_c in 1 T, at 20 K kA/cm ²	N , % ^a
P=2 GPa, T=800 °C, τ =1h	Ta, 10%	240	12.5
	Ti, 10%	360	14
	without	131	10.8

^a The amount of the “black” inclusions, N , was calculated as a ratio of the area occupied by the “black” inclusions at the COMPO image obtained at 1600x magnification to the total area of this image.

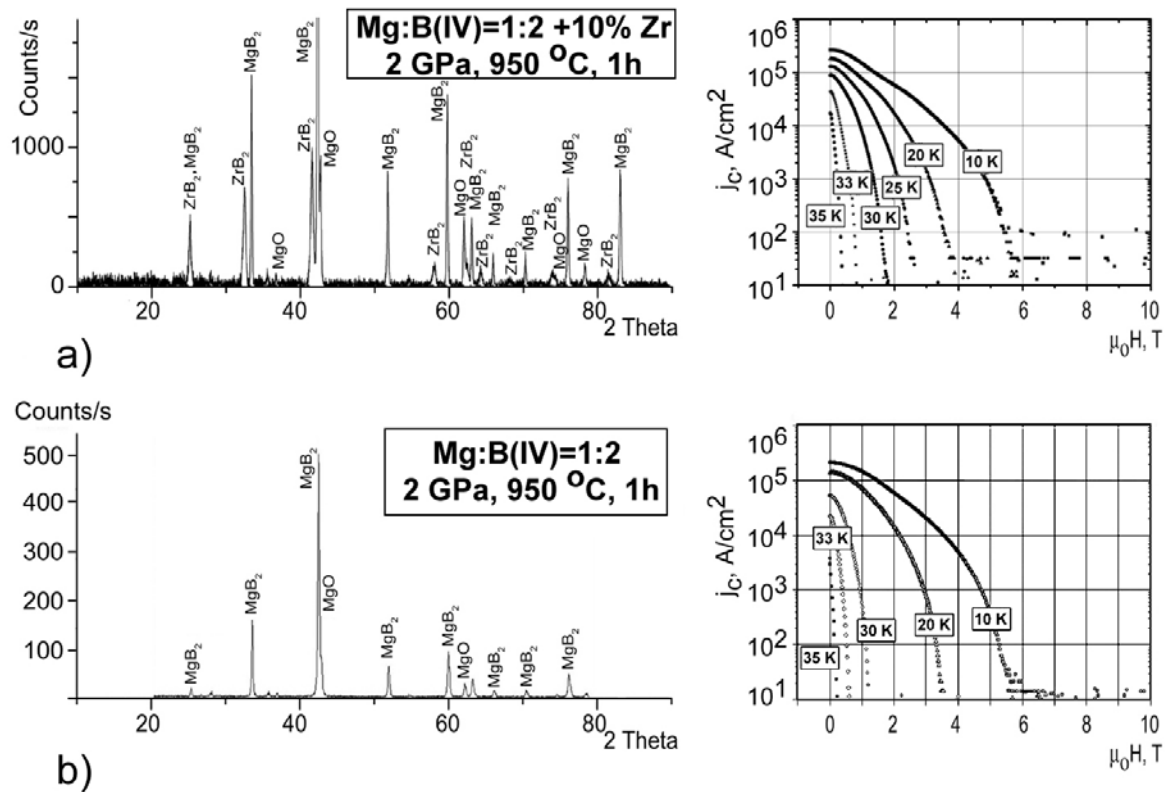


Figure 4. X-ray patterns and dependences of critical current density, j_c , on magnetic fields, $\mu_0 H$, for HPS-materials at 2 GPa, 950 °C for 1 h from Mg:B(IV) with 10 wt% Zr (a) and without additives(b).

energy detector. Quantitative TEM-EDX analysis of boron was performed using the Oxford INCA energy program, 0.7 nm probe diameter.

The average crystallite sizes from line broadening in X-ray diffraction pattern were calculated by the standard program in accordance with the following:

$$\text{Crystallite size} = \frac{K \cdot \lambda}{W_{\text{size}} \cdot \cos \theta} \quad \text{with} \quad W_{\text{size}} = W_b - W_s \quad (1)$$

where W_{size} is the broadening caused by small crystallites; W_b is the broadened profile width; W_s is the standard profile width (0.08 °); K is the form factor; λ is the wavelength.

The values of j_c were estimated by an Oxford Instruments 3001 vibrating sample magnetometer (VSM) using Bean's model. Hardness was measured using a Matsuzawa Mod. MXT-70 microhardness tester, H_V (using a Vickers indenter) and Nano-Indenter II, H_B (using a Berkovich indenter).

3. Results and discussions

3.1. Structural factors which affect pinning and j_c of MgB₂-based materials.

There are many structural factors which can influence pinning and j_c of MgB₂-based materials and it is very difficult to separate one factor from the others and to study the effect of the only definite one. Despite the comparatively simple MgB₂ crystallographic structure (hexagonal lattice) the structures of MgB₂-based materials are very complicated (see, for example Fig. 5 b). It is difficult to study correlations between the structure and j_c first of all because of the nanosized grains of the main

(matrix) phase and due to the fact that oxygen and hydrogen can easily incorporate into the material structure (the amount and distribution of them can essentially affect the SC characteristics). It is difficult to avoid the oxygen and hydrogen presence because MgB₂-based materials as well as initial B and Mg possess a high reactivity toward oxygen and hydrogen. Besides, the boron has a low X-ray atomic scattering factor [8] and even dealing with near theoretically dense materials it is not easy to estimate the amount of boron by energy-dispersive analysis even using high resolution TEM and SEM. We cannot detect the presence of MgB₁₂ in MgB₂ structure by X-ray due to weak diffraction signals (Figs. 5c, d) likely because MgB₁₂ phase is dispersed in the matrix material. Besides, the etalon X-ray pattern of MgB₁₂ is absent in the database and the literature data are contradictive: some researches considered that MgB₁₂ has hexagonal (or rhombohedral) lattice [9, 10] and the other ones that it is orthorhombic [11]. There still exists vagueness concerning appearance, composition and structure of higher boride phases (MgB₄, MgB₆ or MgB₇, MgB₁₂, MgB₁₆ or MgB₁₇ and MgB₂₀). Figures 5a, b, e can be the illustration of MgB₁₂ effect on j_c . The material sintered from MgB₂ contained much less grains with near MgB₁₂ stoichiometry (than that synthesized from Mg:B(I)=1:2 (Fig. 5b), which may affect j_c (Fig. 5e), but the presence of this phase is not reflected in the X-ray pattern (Figs. 5c, d).

Our attempts to find correlations between the average grain size, oxygen content of the initial materials (B or MgB₂ powders) and the amount of oxygen in high-pressure-synthesized (so called *in-situ*) or sintered (so called *ex-situ*) magnesium diboride as well as with j_c of these materials failed (Figs. 6, 7, Table 2). As is seen from Fig. 6 there is no correspondence between the oxygen content in starting boron or MgB₂, its amount in the material obtained and j_c , for example, at 20 K in 1T field. The average crystallite sizes as were shown by the calculations from the line broadening in the X-ray diffraction pattern increased with temperature (Table 2) especially for *in-situ* produced MgB₂, but the variation of j_c does not correspond to variation in grain sizes. In low magnetic fields the critical current density of the *in-situ* prepared MgB₂ increases with increasing synthesis temperature from 800 °C to 1000 °C or increasing crystallite sizes from 15 to 37 nm, but in high or higher magnetic fields the opposite tendency is observed (Fig. 7). Besides, the values of j_c of *in-situ* synthesized at 900 °C material with intermediate sizes of crystallites of 21 nm (Table 2) demonstrated the values j_c lower than those of synthesized at 800 °C in investigated area (at temperatures from 10 to 35 K and magnetic fields 0 - 10 T).

Up to now the highest j_c for high pressure-synthesized MgB₂-based materials in magnetic fields up to 9, 6, and 4.2 T at 10, 20, and 25 K, respectively were exhibited materials prepared at 2 GPa, 1050 °C for 1 h (Fig. 8c, solid symbols) from Mg and B(II) with 10 % of SiC (200-800 nm). But at higher temperatures, 30-35 K, up to 2-1 T fields the highest j_c were for material synthesized from the same boron B(II) under the same conditions but without additives (Fig. 8d, solid symbols). The highest j_c in magnetic fields higher than 9 T, 6 T, and 4.2 T at 10 K, 20 K, and 25 K were exhibited by materials HP-synthesized only at 600 °C from HyperTech produced Mg(A) and B(V) also without additives (Fig. 8d, open symbols). It should be mentioned that the last-mentioned material at 20 K showed $j_c = 10^2$ A/cm² in 10 T field, which is 100 times higher than that reported for material with SiC additive in [12]: “The irreversibility field (H_{irr}) for the SiC doped sample reached the benchmarking value of 10 T at 20 K, exceeding that of NbTi at 4.2 K”.

3.2. Structure and properties of high-pressure synthesized MgB₂-based materials with additions of SiC, Ti, Ta.

As it is pointed out in [12] “a comparative study of pure, SiC, and C doped MgB₂ wires has revealed that the SiC doping allowed C substitution and MgB₂ formation to take place simultaneously at low temperatures. C substitution enhances H_{c2} , while the defects, small grain size, and nanoinclusions induced by C incorporation and low-temperature processing are responsible for the improvement in J_c ”. In the case of HPS materials we failed to improve j_c using nano SiC additive with particle sizes of 20-30 nm as well as by adding SiC with particle sizes of 200-400 nm (Fig. 9). The only some improvement of j_c was observed at 10 and 20 K in high magnetic fields (above 7 and 4 T, respectively)

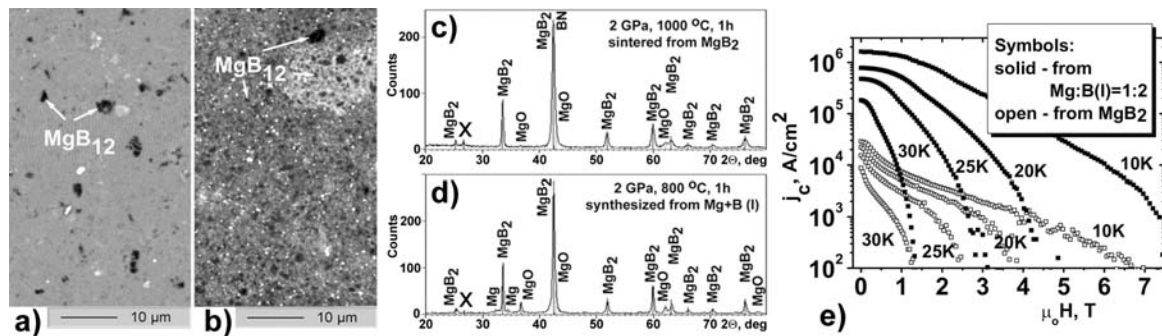


Figure 5. (a), (b) structures of the samples obtained by SEM in COMPOsitional contrast: (a) sintered from MgB_2 at 2 GPa, 1000 °C, 1 h; (b) synthesized from Mg and B taken into 1:2 ratio at 2 GPa, 800 °C: bright small inclusions in Fig. 5b seem to be inclusions because of milling (containing O, Zr and Nb, possibly ZrO_2), which were in the initial boron; bright bigger inclusions are unreacted Mg; (c), (d) –X-ray patterns of the samples shown in Figs. 5a, b; (e) dependences of critical current density, j_c , on magnetic fields, $\mu_0 H$, at different temperatures of the samples shown in Figs. 1a, b: open symbols – sintered from MgB_2 material and solid symbols - synthesized from Mg and B (I) taken into 1:2 ratio.

with nano SiC (20-30 nm) doping (Fig. 9a). The comparison of X-ray patterns (Figs. 8a, 9a-c) as well as SEM study witnessed that the improvement in j_c in the case of HPS materials was obtained when it was no notable interaction between SiC and MgB_2 (Fig. 8a) i.e. in the case when coarse-grained SiC of 200-800 nm was used. But when this interaction took place (Figs. 9a, b) there were usually no improvements or a dramatic reduction of j_c at 30-35 K even occurred. According to our results the pinning centers in SiC doped MgB_2 which influenced j_c increase (compare Figs. 8b, d) may be SiC grains by themselves, inclusions of higher borides (MgB_{12}) and Mg-B-O inclusions enriched with oxygen as compare to oxygen content in the matrix phase (Figs. 10 g, h). The better SC properties can be reached when there is no reaction (detectable by X-ray) between SiC and MgB_2 . So, it is most likely that the improvement in j_c in HPS SiC-doped material is due to the formation of nanostructural inhomogenities in MgB_2 matrix and presence of small SiC grains than due to carbon incorporation in MgB_2 crystal structure.

Figures 10 a-i show the structures of the materials high pressure synthesized from magnesium and different boron types taken in MgB_2 stoichiometry at 600, 800, and 1050 °C without and with Ti, Ta, and SiC additives. The matrix of all samples contained Mg and B in near- MgB_2 stoichiometry and some oxygen (5-10 wt.%), because of this it was marked as Mg-B-O. Oxygen in MgB_{12} inclusions was practically absent, 0.2-1.2 wt.%. Structural observations showed that at a synthesis temperature of about 800 °C oxygen is comparatively homogeneously distributed in the matrix material (Figs. 10a, c), but as the synthesis temperature increases, the distribution of oxygen in the matrix is less homogeneous: the oxygen-enriched (as compared to the amount of oxygen in the matrix) areas form (Figs. 2b, 10b) and with addition of Ta or Ti such areas are transformed into separate Mg-B-O inclusions (light or white inclusions in Figs. 10 d-h). All materials also contain black inclusions with near- MgB_{12} stoichiometry, the amount of which decreases with increasing the synthesis temperature, and increases with addition of Ta or Ti. In our opinion both MgB_{12} and Mg-B-O inclusions can positively affect pinning in MgB_2 . As it was mentioned above our previous studies showed that after HP-synthesis Ta and Ti in many cases (especially when j_c increased) transformed into Ta_2H or $\text{TiH}_{1.924}$ hydrides and never into oxides. But up to now we have not fully understood the mechanism of Ti or Ta influence the on j_c increase (compare Figs. 1a, b, 8i, f) in MgB_2 -based materials. We can assume that the existence of the two so-called optimal temperatures for the same starting boron may be the result of competition between higher borides (MgB_{12}) formation and oxygen segregation to form Mg-B-O inclusions. When studying oxygen content we found that gray matrix of material high pressure

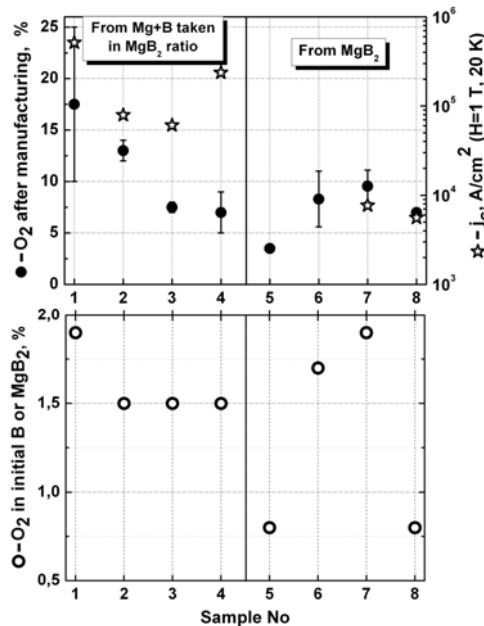


Figure 6. The amount of oxygen in the initial boron or MgB_2 powder (\circ) and in the prepared (\bullet) materials (synthesized from Mg and B taken in 1:2 ratio or sintered from MgB_2) and critical current density (\star) in 1 T field at 20 K estimated using VSM in different samples manufactured at 2 GPa for 1h at 800 °C (Nos 1, 2, 5), 900 °C (Nos 3, 6, 7) and 1000 °C (Nos 4, 8). The shape of hysteresis loops of samples 5 and 8 witnessed the absence of connectivity between the superconductive grains in the materials, thus as a whole the materials were not superconductive. The sample 1 prepared from boron with average grain size of 1.4 μm , samples 2, 3, 4 from 4 μm boron and samples 5 and 8 from 10 μm , sample 6 from 9 μm , sample 7 from 1.4 μm MgB_2 .

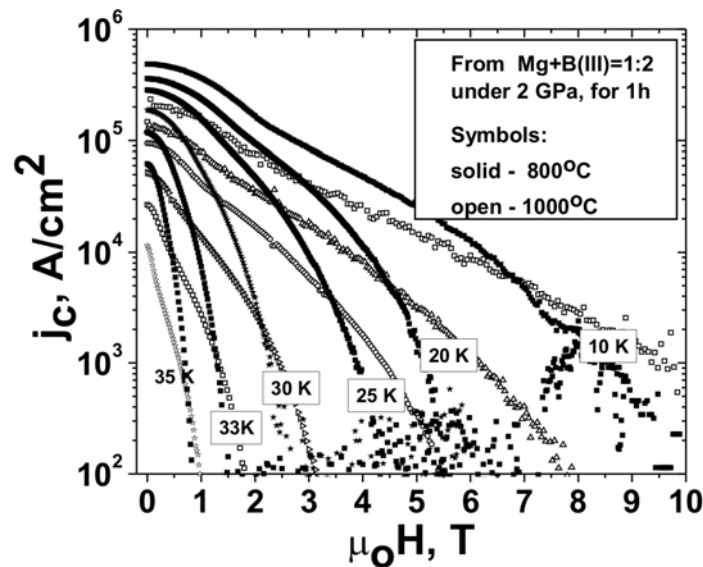


Figure 7. Dependences of critical current density, j_c , at different temperatures on magnetic fields, $\mu_0 H$, for HPS-materials at 2 GPa for 1h from $\text{Mg}:\text{B(III)}=1:2$ at 800 °C (open symbols) and 1000 °C (solid symbols).

Table 2. Critical current density, j_c , vs. relative average grain size of crystallites of high-pressure sintered from MgB_2 and synthesized from Mg and B(III) taken in 1:2 ratio materials.

HPS under 2 GPa for 1 h at T_s , °C	average crystal size	lattice parameters		j_c , kA/cm ² at 10 K		j_c , kA/cm ² at 20 K	
		a (nm)	c (nm)	0 T	1 T	0 T	1 T
From MgB_2							
700	19.7 nm	0.30805	0.35188	-	-	-	-
800	18.8 nm	0.30822	0.35212	-	-	-	-
900	18.5 nm	0.30820	0.35208	56	14	36	8
1000	25.0 nm	0.30797	0.35200	28	8	19	5
From Mg and B (III) in 1:2 ratio							
800	15.0 nm	0.30747	0.35188	245	142	138	79
900	21.0 nm	0.30819	0.35174	205	136	128	61
1000	37.0 nm	0.30808	0.35192	485	364	360	237

synthesized at 800 °C with 10 % of Ti contained 8 % of oxygen, while gray matrix (between bright oxygen-enriched inclusions) of the materials high pressure synthesized from the same B and Mg at 1050 °C with addition of 10% Ti or Ta contained only 1.5 - 5 or 6 % oxygen, respectively. So, Ti and Ta seem to promote a decrease of oxygen amount in the matrix material, thus contributing to the formation of Mg-B-O inclusions with high oxygen content and pinning increase. The segregation of oxygen with temperature increase in materials without additions is not so pronounced.

Such high critical current densities in high magnetic fields (Figs. 8c, open symbols) exhibited by material synthesized at very low temperature 600 °C (from Mg(A) powder and B(V)) were very unusual for our previous studies. The structure of this material was not very dense and rather inhomogeneous (Fig. 10 i). Up to now this material has not been studied properly, we can only assume that there is near 7 wt% of oxygen in its matrix and the composition of the matrix corresponds approximately to $MgB_3O_{0.3}$. As our former results have shown the substitution of Mg chips for 325 meshes powdered Mg did not allow us to improve j_c and the use of synthesis temperature below 800 °C resulted in the absence of SC properties or in very low values of j_c .

3.3. Formation and properties of higher borides.

The notable effect of the presence of MgB_{12} phase inclusions in MgB_2 on SC properties compelled us to focus our attention on MgB_{12} synthesis. For this study we used only boron B(III) and Mg chips (the mixtures were mixed and milled in a high-speed activator). Our multitudinous studies allow us to conclude that appearance of reflex “x” (Figs. 5c, d, 9a, b) or reflexes “3” (Fig. 11g) on X-ray can be responsible for higher borides (this reflex exactly corresponds to hexagonal BN, which is used to protect samples from a graphite heater, but the samples under study contain no nitrogen). Figures 11a-e demonstrate (using backscattering electron regime) the essential difference between materials with MgB_2 (Figs. 11a-d) and MgB_{12} (Fig. 11e) matrixes. As is shown from high-resolution TEM studies, MgB_{12} grains (Fig. 11f) were far from perfection and contained many mosaic subgrains. The last mentioned reason can be an explanation to the fact why we did not get sharp reflections of Kikuchi lines from MgB_{12} grains.

The specially HP-synthesized samples from mixtures with a large amount of boron (up to Mg:B=1:20) exhibited SC properties (Fig. 11h). The highest j_c as well as T_c near 37 K were demonstrated by samples with near MgB_{12} composition of matrix (prepared from mixtures Mg:B= 1:8) whose structure and properties are shown in Figs. 11e, f, g, i, j. The corrected amount of shielding fraction in the sample is 95.3% which witnesses a large volume of SC phase. As high-resolution TEM

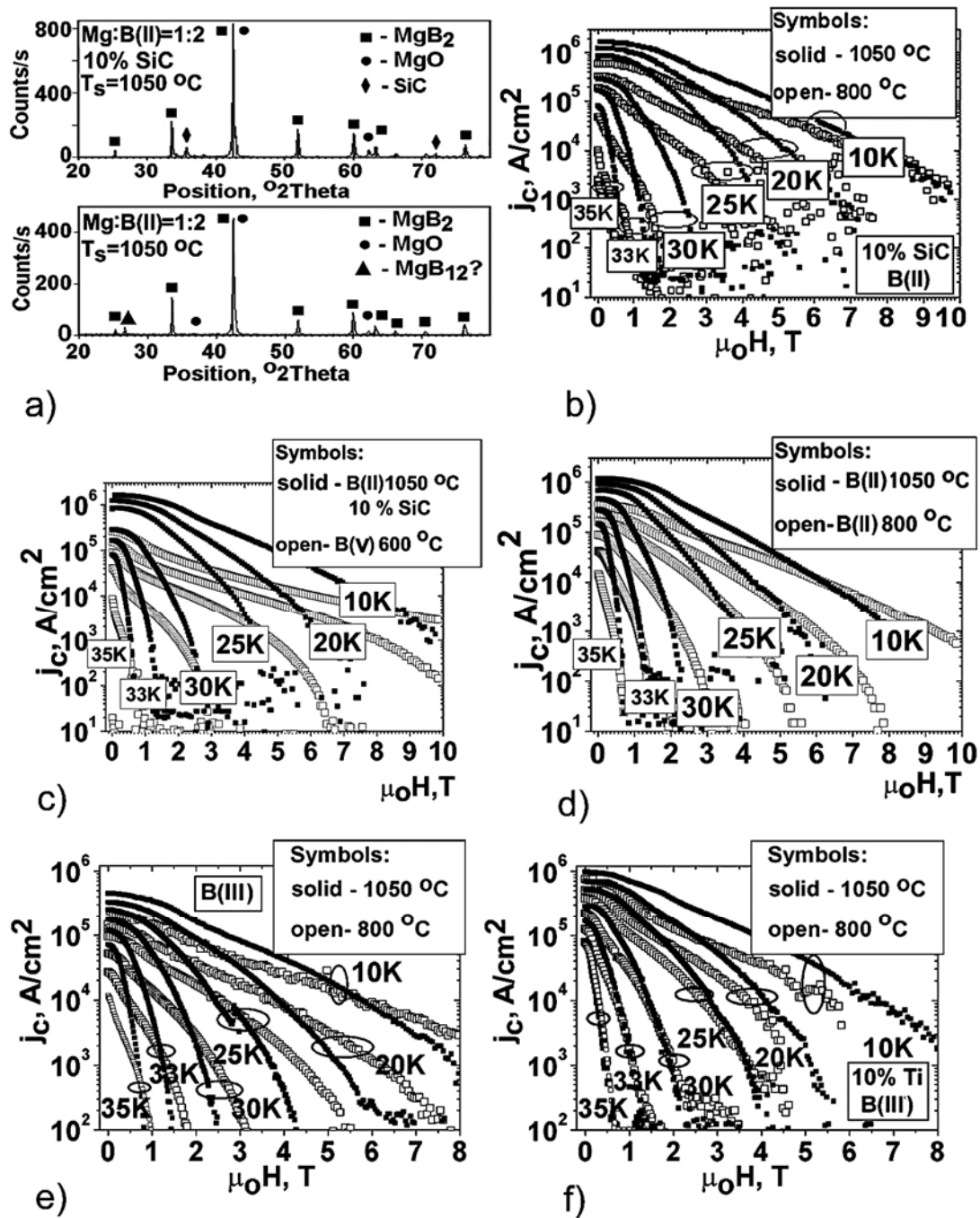


Figure 8. (a) X-ray patterns of materials synthesized from Mg and B(II) taken into 1:2 ratio at 2 GPa, 1050 °C for 1h with SiC additive (upper picture) and without additive (lower picture); (b-f) dependences of critical current density, j_c , at different temperatures on magnetic field, $\mu_0 H$, for HPS-materials at 2 GPa for 1h: (b) from Mg:B(II)=1:2 with 10% SiC (200-800 nm) at 800 °C (open symbols) and 1050 °C (solid symbols), (c) from Mg:B(II)=1:2 with 10% SiC (200-800 nm) at 1050 °C (solid symbols) and from Mg(A):B(V)=1:2 at 600 °C (open symbols), (d) from Mg:B(II)=1:2 at 800 °C (open symbols) and 1050 °C (solid symbols), (e) from Mg:B(III)=1:2 at 800 °C (open symbols) and 1050 °C (solid symbols), (f) from Mg:B(III)=1:2 with 10% Ti at 800 °C (open symbols) and 1050 °C (solid symbols).

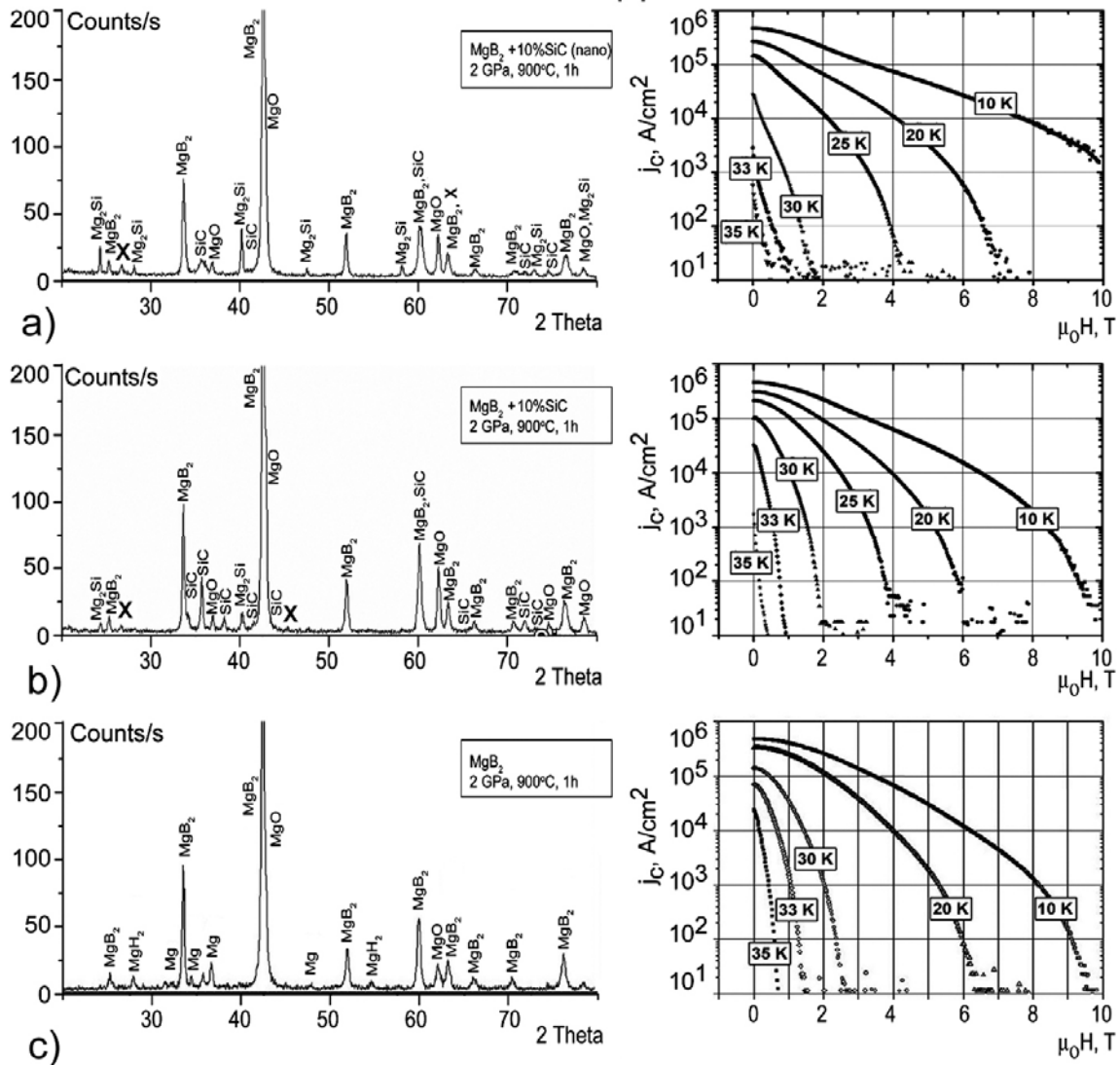


Figure 9. X-ray patterns and dependences of critical current density, j_c , at different temperatures on magnetic field, $\mu_0 H$, for HPS-materials from Mg:B(IV)=1:2 at 2 GPa, 900 °C, 1 h: (a) with 10% nano SiC additive with particle sizes of 20-30 nm, (b) with 10% SiC additive with particle sizes of 200-400 nm, (c) without an additive.

and SEM energy-dispersion analysis showed, the sample (Fig. 11e) mainly contained a phase with near MgB₁₂ stoichiometry and some amount of MgB_(5.3-6.8) (MgB₂ was found in the form of random inclusions of less than 100 nm). A high j_c were shown by the material synthesized from Mg:B=1:20 in which a high amount of SC phase also has been observed and the matrix of which as SEM study revealed had near MgB₁₂ composition. It should be mentioned that the materials with near MgB₁₆ stoichiometry of the matrix exhibited very low SC properties.

The Berkovich nanohardness and Young modulus of the MgB₁₂ inclusions as estimated under the 10-60 mN-load were 32.2±1.7 and 385±14 GPa, respectively, while for sapphire 31.1±2.0 and 416±22 GPa, respectively, and for the Mg-B-O matrix phase (with Mg:B ratio approximately equal 1:2) the Berkovich nanohardness and Young modulus were 17.4±1.1 and 213±18 GPa, respectively. The Vickers microhardness under 4.9 N-load of HPS sample with near MgB₁₂ matrix (Fig. 11 f) was 25.6±2.4 GPa and with near MgB₂ one was 13.08±1.07 GPa.

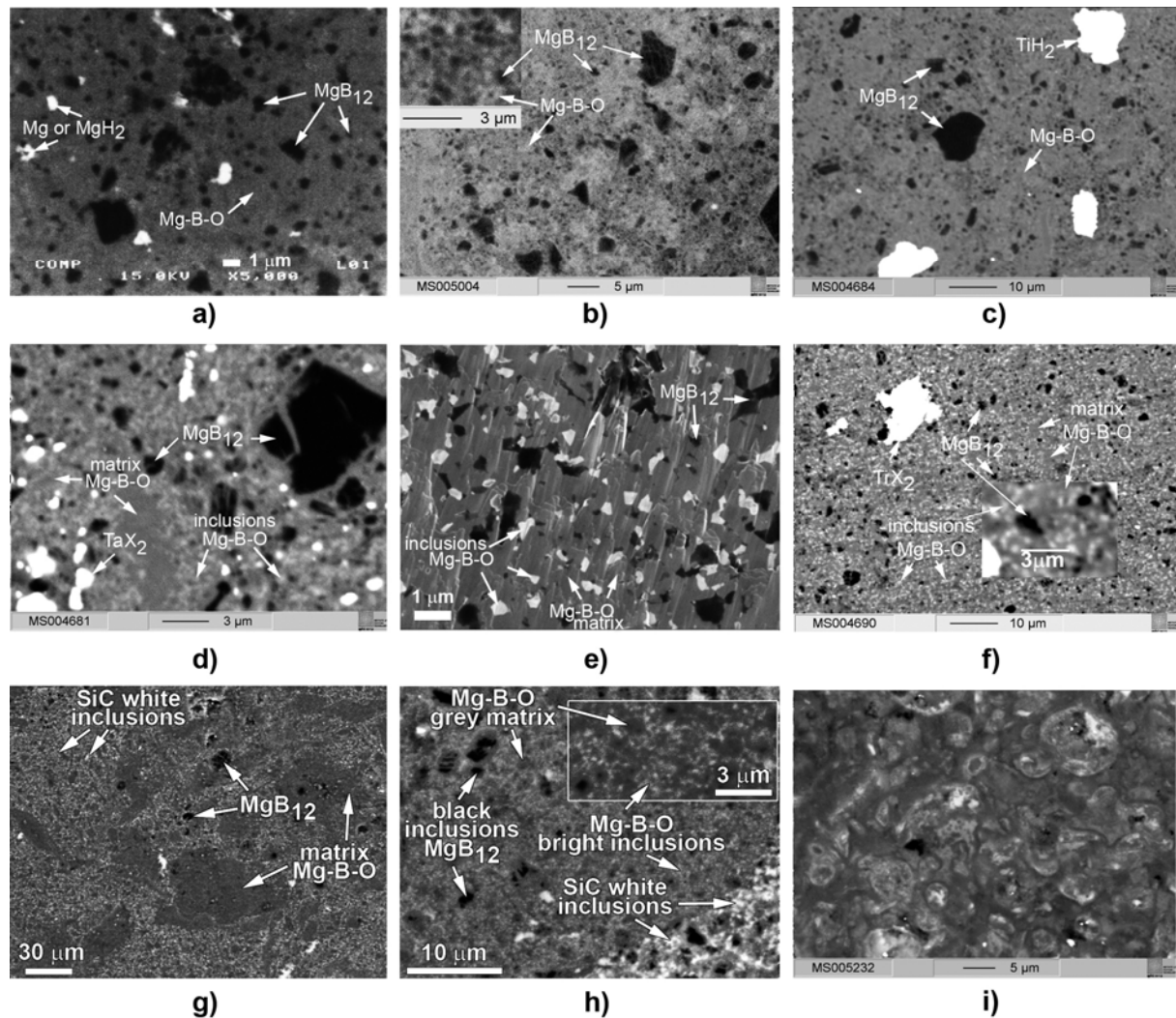


Figure 10. Composition images (backscattering electron images) of HPS MgB_2 -based materials (a-h) synthesized from Mg and B taken in MgB_2 stoichiometry at 2 GPa for 1 h: (a) at 800 °C from boron B(IV); (b) at 1050 °C from boron B(III) (c) at 800 °C with 10% Ti from boron B(III), (d) at 1050 °C with 10% Ta from boron B(III), (e, f) at 1050 °C with 10% Ti from boron B(III) under different magnifications (Fig. 10e shows the enlarged area containing no Ti, the “steers” seen in matrix are because of etching), (g, h) at 1050 °C with 10% SiC (200-800 nm) from boron B(II) under different magnifications (Fig. 10h shows the enlarged area containing small amount of SiC); (i) synthesized from $\text{Mg(A)}:\text{B(V)}=1:2$ at 2 GPa, 600 °C for 1 h.

So, careful structural studies using high resolution SEM and TEM, microhardness tests (which showed that MgB_{12} phase is as hard as sapphire) pointed to a principal difference between samples prepared from $\text{Mg}:\text{B(III)}=1:8$ ratio and MgB_2 -based materials. The foregoing allows us to conclude that in materials with near MgB_{12} matrix the comparatively high critical current densities can be realized.

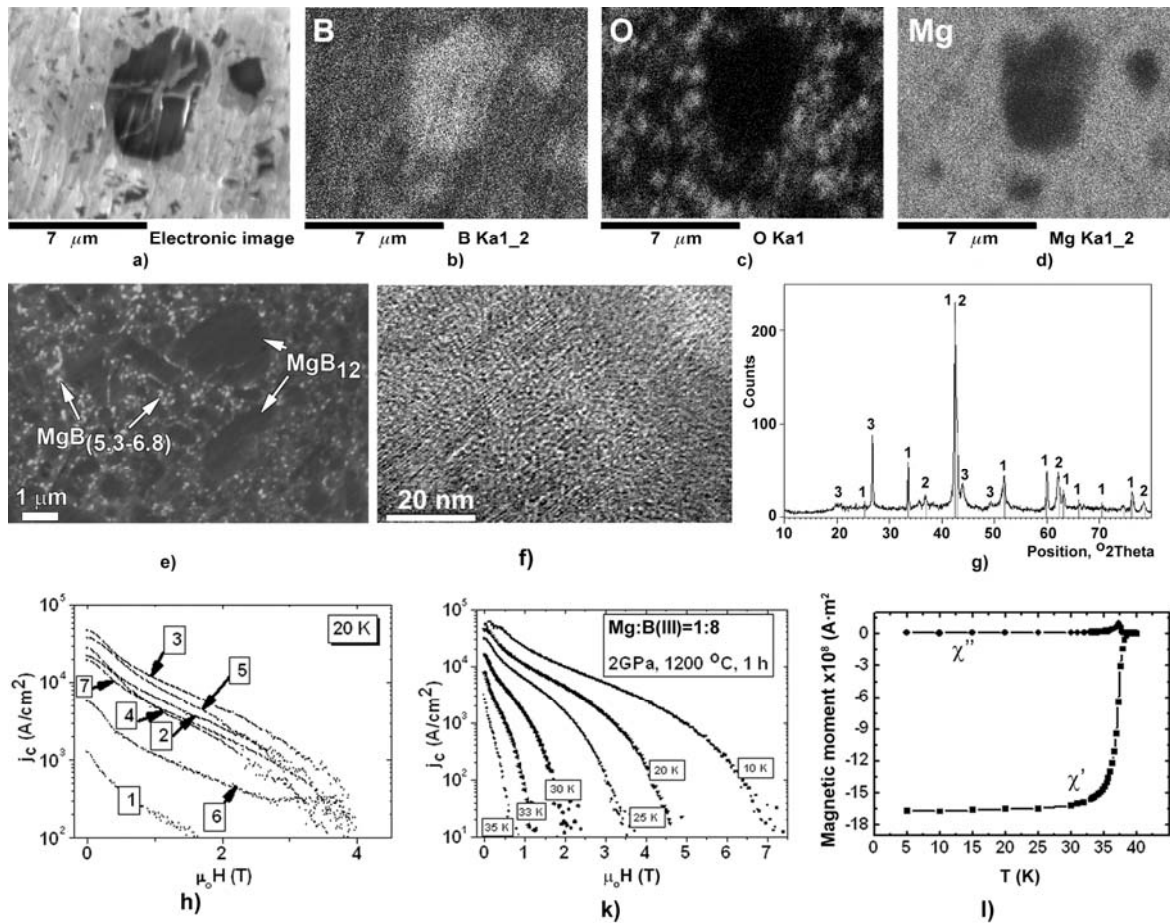


Figure 11. (a-d) backscattering electron image and analysis of elements distribution (the brighter looks area the higher is amount of the element under study) over the area of HPS MgB₂-based sample from Mg and B(III) with 10% Ti taken in MgB₂ stoichiometry at 2 GPa, 1050 °C, for 1 h: (a) electron image, (b - d) distribution of boron, oxygen and magnesium, respectively (the same sample is shown in Figs. 10e, f); (e, f, g, i, j) views of structure and characteristics of the material synthesized from Mg and B(III) taken into 1:8 ratio at 2 GPa, 1200 °C for 1 h: (e) backscattering SEM electron image: the stoichiometry of matrix is near MgB₁₂, (f) TEM image which shows the mosaic structure of a MgB₁₂ grain; (g) X-ray pattern of the sample (reflexes “1” and “2” coincide with those of MgB₂ and MgO, respectively, reflexes “3” possibly belong to MgB₁₂, reflex “3” at 2θ=27° coincides with that of BN), (i) dependences of critical current density, j_c , on magnetic fields, $\mu_0 H$, (j) dependences of real (χ') and imagine (χ'') parts of resistance vs. temperature; (h) dependences of j_c on the external magnetic fields, $\mu_0 H$, at 20K for the materials synthesized at 2 GPa for 1 h from Mg and B(III) taken in the ratio Mg:B and synthesized at T_S : curves 1 - 1:12, $T_S = 1200$ °C, curve 2 - 1:10, $T_S = 1200$ °C, curve 3 - 1:8, $T_S = 1200$ °C, curve 4 - 1:6, $T_S = 1200$ °C, curve 5 - 1:4, $T_S = 1200$ °C, curve 6 - 1:12, $T_S = 800$ °C, curve 7-1:20, $T_S = 1200$ °C.

4. Conclusions

The SC properties of MgB₂-based materials depend to a large extend on the distribution of nanostructural inhomogenities with higher boron and oxygen contents (higher borides and Mg-B-O inclusions) as well as on the presence of hydrogen, which in turn depend to a high extent on the quality of initial boron or magnesium diboride powders and can be regulated by synthesis or sintering temperatures and by the type and amount of alloying additives such as Ti, Ta, SiC, etc.

At low synthesis temperatures (about 800 °C) the presence of Ti or Ta promotes the formation of MgB₁₂ inclusions, which positively affects pinning in MgB₂-based materials, especially in high magnetic fields. Under high synthesis temperatures (about 1050 °C) adding of Ti and Ta seems promotes a decrease of the amount of oxygen in the matrix material by contributing to the formation of inclusions with a high oxygen content (Mg-B-O – inclusions) which can act as pinning centers as well. The segregation of oxygen and formation of Mg-B-O inclusions with an increase of synthesis temperature in materials without additives are not so pronounced. The better SC properties can be reached when it is no notable reaction between SiC and MgB₂. Probably the improvement in j_c in high pressure-synthesized SiC-doped material is due to the formation of nanostructural inhomogeneties in the MgB₂ matrix and due to the presence of dispersed small SiC grains.

There are many grounds to assume that in materials with MgB₁₂ matrix high SC properties can be attained as in the case of MgB₂ matrix.

5. References

- [1] Prikhna T A, Gawalek W, Savchuk Ya M, Kozyrev A V, Wendt M, Melnikov V S, Turkevich V Z, Sergienko N V, Moshchil V E, Dellith J, Ch. Schmidt, Dub S N, Habisreuther T, Litzkendorf D, Nagorny P A, Sverdun V B, Weber H W, Eisterer M, Noudem J and Dittrich U 2009 *IEEE Transactions on Applied Superconductivity* **19** 2780
- [2] Prikhna T, Gawalek W, Savchuk Ya, Sergienko N, Moshchil V, Dub S, Sverdun V, Kovalev L, Penkin V, Rozenberg O, Zeisberger M, Wendt M, Fuchs G, Grovenor Ch, Haigh S, Melnikov V and Nagorny P 2006 *Advances in Science and Technology* **47** 25
- [3] Klie R F, Idrobo J C, Browning N D, Serquis A, Zhu Y T, Liao X Z and Mueller F M 2002 *Appl. Phys. Lett.* **80** 3970
- [4] Prikhna T A, Gawalek W, Savchuk Ya M, Habisreuther T, Wendt M, Sergienko N V, Moshchil V E, Nagorny P, Schmidt Ch, Dellith J, Dittrich U, Litzkendorf D, Melnikov V S and Sverdun V B 2007 *Supercond. Sci. Technol.* **20** S257
- [5] Hoerhager N, Eisterer M, Weber H W, Prikhna T, Tajima T and Nesterenko V F 2006 *Journal of Physics: Conference Series* **43** 500
- [6] Goto D, Machi T, Zhao Y et al. 2003 *Physica C* **392–396** 272
- [7] Haigh S, Kovac P, Prikhna T, Savchuk Ya M, Kilburn M, Salter C, Hutchison J, Grovenor C 2005 *Supercond. Sci. Technol.* **18** 1190
- [8] Birajdar B, Peranio N, and Eibl O, 2008 *Supercond. Sci. Technol.* **21**, 073001
- [9] Schmitt R 2006 *Dissertation am Institut für Anorganische Chemie, University of Tübingen*, «Binare und ternare Boride der Erdalkalimetalle -Synthesen, Kristallstrukturen und Eigenschaften» unter der Anleitung von Prof. Dr. Meyer H-J.
- [10] Schmit R, Glaser J, Wenzel T, Nickel K G and Meyer H-Jurgen 2006 *Physica C* **436** 38
- [11] Adasch V. 2005 *Dissertation am der Fakultät für Biologie, Chemie und Geowissenschaften der Universität Bayreuth* «Synthese, Charakterisierung und Materialeigenschaften borreicher Boride und Boridcarbide des Magnesiums und Aluminiums» unter der Anleitung von Prof. Dr. Harald Hilleb
- [12] Dou S X, Shcherbakova O, Yeoh W K, Kim J H, Soltanian S, Wang X L, Senatore C, Flukiger R, Dhalle M, Husnjak O and Babic E, 2007 *Phys. Rev. Lett.* **98** 097002